Physiological and transcriptomic variability indicative of differences in key functions within a single coral colony

Jeana L. Drake[1+], Assaf Malik[1+], Yotam Popovits[1+], Oshra Yosef[1], Eli Shemesh[1], Jarsoław Stolarski[2], Dan Tchernov[1], Daniel Sher[1*] and Tali Mass[1*]

[1]Department of Marine Biology, University of Haifa, 199 Aba Koushy Avenue, Haifa, Israel, 3498838
[2]Institute of Paleobiology, Polish Academy of Sciences, Twarda 51/55, Warsaw, Poland, 00-818
+These authors contributed equally
[*]Corresponding authors

Running Head
Coral intracolonial biological variation

Abstract

Polyps in different locations on individual stony coral colonies experience variation in numerous environmental conditions including flow and light, potentially leading to transcriptional and physiological differences across the colony. Here, we describe high-resolution physiological measurements and differential gene expression from multiple locations within a single colony of *Stylophora pistillata*, aiming to relate these to environmental gradients across the coral colony. We observed broad transcriptional responses in both the host and photosymbiont in response to height above the substrate, cardinal direction, and, most strongly, location along the branch axis. Specifically, several key physiological processes appear more active toward branch tips, including toxin production for prey capture or defense, several metabolic pathways, and biomineralization. Further, the increase in gene expression related to these processes toward branch tips is conserved between *S. pistillata* and *Acropora* spp. The photosymbiont appears to respond transcriptionally to relative light intensity along the branch and due to cardinal direction. These differential responses were observed across the colony despite its genetic homogeneity and likely inter-polyp communication. While not a classical division of labor, each part of the colony appears to have distinct functional roles related to polyps' differential exposure to environmental conditions.

Keywords

Differential gene expression, biomineralization, toxins, host and symbiont

1 Introduction

Coral reefs are one of the most biodiverse ecosystems on Earth, creating shallow-water habitats for a significant number of marine species [1], although they face a suite of anthropogenic stressors with both local and global causes [2-5]. Most stony corals (order Scleractinia), the sessile builders of the reef system, grow as colonies of up to hundreds of thousands of genetically identical polyps formed by budding with colonies ranging in size from centimeters to meters in diameter. The reef-building corals are also host to intracellular symbiotic dinoflagellates, whose photosynthetic activity restricts the scleractinian coral holobiont to the top ~100 m of the ocean and fulfills much of the host's carbon nutritional requirements [e.g., 6]. Nevertheless, uptake of dissolved nutrients and active feeding on particles from the water column both play significant roles as well [e.g., 7, 8] [reviewed in 9], with active predation utilizing toxins produced and delivered by cnidocytes [recently reviewed by 10]. These fixed carbon sources ultimately power the production of the external calcium carbonate skeleton that forms the reef and persists after the animal has died.

While the individual polyps in most corals are genetically identical, each polyp inhabits a distinct location within the colony, which can be morphologically complex (e.g., in the case of branching corals). Thus, it has been suggested that individual polyps within a coral colony are differentially exposed to environmental conditions such as water flow and light availability [e.g., 11, 12], which have distinct effects on coral physiology. These micro-environmental conditions may play a role in feeding capability (i.e. zooplankton; [13]), reproductive success [14], photosynthesis [15, 16], calcification rate [16], and waste removal [17]. For instance, reductions in flow between the colony branches can trap food particles, making it easier for the hunting tentacles of the

polyps to efficiently pull them from the water column [11]. Similarly, differences in light exposure due to the coral's geometric branching leads to self-shading that can reduce light availability by more than 50% and can be an effective mechanism of photoprotection in shallow water [18]. This can lead to fine-scale spatial heterogeneity in photosynthetic parameters between individual polyps, as well as between polyps and the coenosarc, the tissue between polyps through which they communicate [19]. Such plasticity has been observed in changes in gene expression in coral branch tips versus bases across multiple colonies [20], but has not previously been linked, at high spatial resolution, to detailed measurements indicative of relevant environmental parameters and physiology within a single coral colony.

Here we combined high-resolution transcriptomic analysis with field measurements and physiological assays to describe intra-colony plasticity in the Indo-Pacific stony coral, *Stylophora pistillata*. Our whole-genome expression and physiological data are from a single coral colony at three locations along each branch, with each branch taken from a different location within the colony. This high-resolution dataset enables us to resolve, for the first time, variability along three main axes – tip-junction-base, top-bottom and the cardinal direction (figure 1a, b). Each of these axes is associated with changes in gene expression and physiology, which we suggest are due in part to light and current direction and strength. It appears that polyps in the interior of the colony are exposed to relatively stagnant conditions, whereas the colony periphery likely experiences higher flow, light exposure, chances for predation, and requirements for competition and defense leading to the dynamic physiological and transcriptional responses observed here.

2 Methods

Extensive descriptions of all methods can be found in the Supplementary Information.

(a) Sample collection

An *S. pistillata* colony collected from the coral nursery of the Inter-University Institute for Marine Science (IUI), Eilat, Israel was fragmented into three branches each from three horizontal concentric rings (Top, Middle, Bottom) and from all sides of the colony, for a total of nine branches, that were further divided into sections according to their position on the branch (Tip, Junction, Base) and flash-frozen in TRI-Reagent (Sigma) (figure 1; electronic supplementary material, table S1) Five additional branches distributed around the colony were chosen for physiological examination, following the same study parameters and then kept at –80 ˚C.

(b) Oxygen measurements and bacterial counts

Dissolved oxygen (DO) concentrations in seawater between branches of five *S. pistillata* colonies located in the IUI coral nursery were measured as five radial transects per colony, from the center of each colony, mid-way to the periphery, and at 10 cm above each respective colony, using Unisense oxygen microsensors mounted on a Unisense UnderWater Meter System. All measured oxygen concentrations were normalized to 1 ATM (sea surface pressure) and then values for each colony were normalized to the 'inside' value for that colony to achieve a relative DO concentration for locations within each colony. Bacterial counts at 5-7 locations per colony just outside the colonies and within the coral colonies were performed on samples collected in-situ on five different colonies growing at the same site. All water samples were stored at −80 °C in 0.0625% glutaraldehyde until analysis by flow cytometry. Just prior to analysis, thawed bacterial count samples were diluted 1:1 in ultra-pure water with 2 µm-diameter fluorescent beads added to each sample as an internal standard (Polysciences, Warminster, PA, USA) before

analysis of chlorophyll and phycoerythrin fluorescence and SYBR Green staining on a FACSCanto™ II Flow Cytometry Analyzer Systems (BD Biosciences). Data were acquired and processed with FlowJo software.

(c) Tissue analysis

Tissue was removed from the frozen coral fragment skeleton by airbrush and homogenized in phosphate buffered saline (PBS). Sub-samples of each fragment's total homogenate were analyzed for nematocyst and symbiont cell counts by light and fluorescence microscopy, chlorophyll filter-extraction in 90% acetone [21], and homogenate protein measurements. The remainder of the homogenate was centrifuged; the supernatant was analyzed for host protein and hemolysis while the pellet was sonicated and analyzed for symbiont protein. Quantitative hemolytic assays of crude coral tissue extracts were performed against washed O Rh positive human red blood cells (4% erythrocytes v/v) [22] in a three-fold dilution series. HU_{50} was defined as the amount of coral protein required to cause 50% hemolysis [23].

(d) Skeleton analysis

After tissue extraction, all fragments were cleaned of organic residues overnight in 3% sodium hypochlorite, rinsed copiously in deionized water, and dried. Skeleton surface areas of all sectioned fragment were estimated using the aluminum foil method in triplicate [24]. Replicate distances between polyps and polyp surface areas were imaged by binocular microscope and analyzed using NIS-Elements (Nikon) software. Major and minor axes and circularity were measured for each corallite and the ratio of the two axes (major divided by the minor) were calculated; a ratio of 1 indicates a circle and the larger the ratio, the more elliptical the shape. Corallites were qualitatively analyzed by scanning electron microscopy after a water wash, tissue removal by airbrush, overnight drying, fragmenting, and platinum sputter-coating.

(e) RNA extraction, processing, and sequencing

RNA was extracted from fragments stored in Tri-Reagent, purified, and washed in 70% ethanol. Following on-column DNA digestion, RNA libraries were prepared at the Weizmann Institute of Science and sequenced on an Illumina HiSeq 2500.

(f) Differential expression analysis

In order to detect correct taxonomic classifications within our transcriptome data, high-quality RNA-Seq reads were mapped to the selected genome-based predicted proteome databases of the formerly classified *Symbiodinium* spp. (now elevated to family Symbiodiniaceae; [25]), stramenopiles/alveolates/Rhizaria, and Cnidaria/Metazoa from UniRef, NCBI, and Reefgenomics.org using Diamond [26]. Then, RNA-Seq reads were mapped to the merged host genome assembly (NCBI GCA_002571385.1) and the relevant symbiont genome assembly (*Symbiodinium microadriaticum*, NCBI GCA_001939145.1) using STAR [27-29]. In total, 83-84% of the reads were aligned to either host or symbiont genomes. Differential expression (DE) analysis was conducted using Bioconductor DEseq2 [30], separately for the host and the symbiont genes, using DEseq2 (electronic supplementary material, table S2). Due to lower read counts in the symbiont data and in order to achieve balanced distribution of read counts in those data (as indicated in MA plots), genes with a lowest quartile of <12 reads were excluded yielding ~10,000 remaining informative symbiont genes, and only samples with >300k reads total were included. Specifically, we tested: (1) the additive effect of branch position, ring height and cardinal direction; (2) the additive and interaction effect of branch position and ring height (excluding the cardinal direction factor) (see electronic supplementary mater, tables S3, S4, S5). The second model was not tested for photosymbiont genes since the power of such models is limited when the read counts per samples are low. We also note that the additive model (1)

cannot consider the ring Top samples since no cardinal direction factor exists in these four samples. As the additive model output was used for further analysis of putative toxin and known biomineralization-related genes, these samples were excluded in those analyses as well. Sequencing information is available in a read-only format on BioProject (PRJNA640617: https://dataview.ncbi.nlm.nih.gov/object/PRJNA640617?reviewer=ta79noetg8fhsvhebud2uj85d2); data will be made freely available on BioProject upon acceptance of the manuscript for publication. NMDS analysis was conducted using metaDMS in the R Vegan package with Bray Curtis dissimilarity based on $\log_{10}$FPM values of all expressed genes. For the symbiont NMDS, since read counts were relatively low, pairs of tips from the same branch are represented together based on the sum of read counts for both tips.

(g) Branch genetics and SNPs analysis

Single nucleotide polymorphisms (SNPs) analysis was conducted for each sample using the Broad Institute-recommended RNA-Seq SNPs practice (https://gatk.broadinstitute.org) by STAR reads mapping, removing various alignment biases, variant calling using GATK version 3.5, and finally variant filtration and annotation [31]. We considered only SNP loci with coverage greater than 30 RNA-Seq reads in all tested samples. Identity By Decent (IBD) analysis was conducted using SNPRealte in R.

(h) Host and symbiont functional enrichment analysis

Biological terms were assigned to genes based on UniProt *S. pistillata* (www.uniprot.org), KEGG *S. pistillata* (www.kegg.jp), *S. pistillata* Trinotate annotations [32], and UniProt *S. microadriaticum* databases. Host KEGG term enrichment reflects concrete and relevant gene functions. However, low read counts for the photosymbiont required gene set enrichment analysis (GSEA) which is dependent on GO terms. Enrichment analysis was conducted in

Bioconductor GOSeq [33] and using the score-based gene set enrichment analysis tool [34, 35] using $\log_2$ fold changes ($\log_2$FC) as scores. We then hierarchically clustered the biological terms based on pairwise distances between groups of genes. Terms trees were constructed using Bioconductor-ggtree [36].

(i) Environmental and Physiological Statistics

Statistical tests of all skeletal, physiological, and environmental data were performed in RStudio [37]. If a parameter displayed both homogeneity of variance (Fligner-Killeen test) and normal distribution (Shapiro-Wilke test), either a t-test or a one-way ANOVA was performed, with TukeyHSD post hoc analysis for parameters with significant differences between branch locations. Parameters with non-homogenous variance and/or non-normal distribution were analyzed using Wilcoxon's rank sum test or the Kruskal-Wallis rank sum test, with Dunn's test for post hoc analysis for parameters with significant differences between branch locations.

3 Results and Discussion

(a) Differences in dissolved oxygen and microbial counts in water across colony structure

Branching corals' three-dimensional structure can lead to different micro-environments within the colony. We therefore first aimed to characterize indicators of the environmental conditions experienced by polyps at different locations within the coral colony, that could potentially affect their gene expression. We examined five colonies of *S. pistillata* in-situ (at depths of ~5 m) and focused on the water column characteristics of oxygen concentration, which has been shown to vary within colonies and affect coral physiology [17], and bacterial counts. We chose these parameters because, unlike flow fields, both are easily quantifiable properties related to interstitial water column stability. As shown in figure 1c, we measured higher oxygen

concentrations in water collected close to the core (interior) of the corals, compared to samples collected towards the colony peripheries ($p<0.05$, Wilcoxon rank sum test; electronic supplementary material, tables S6, S7). We also observed higher microbe densities in water collected from the colony interiors versus the immediately surrounding seawater (figure 1d, $p<0.05$, Wilcoxon rank sum test; electronic supplementary material, tables S6, S7). Both of these observations may be due to lower rates of water exchange at the base of the branches due to decreased water flow within the colony, as suggested by [11]. Further, coral branch density has been found to affect intercolonial water flow, with lower mass transport for the less densely branched *Pocillopora eydouxi* whose overall colony structure is similar to the *S. pistillata* studied here (figure 1a) compared to the more densely branched *P. meandrina* [38]. Flow reduction within the colony would cause the accumulation of oxygen produced by photosynthesis [17] and we speculate might also support the retention of microbes actively growing between branches [39], or those chemotaxing toward the coral tissue [40]. Higher microbial densities between the polyps at the interior of the colonies might enable polyps to feed directly on the bacteria or on bacterial predators [39, 41], and mucus release by the corals [42, 43] could provide organic carbon for the growth of microorganisms, further maintaining feedbacks between the coral, flow, and these water-column microbes. Diminished flow in the interior of the colonies could also result in increased interactions with various infectious organisms that target the oral ectoderm [e.g., 44], leading to diseases such as skeletal band eroding disease [45], which has been observed to commence at colony interiors. Regardless of the mechanism driving the changes in oxygen concentration and microbial abundance, these differences further support the notion that the environment along the coral branches from colony exterior to interior differs depending on

the morphology of the coral and may affect the coral holobiont with some polyps inhabiting more or less favorable areas.

(b) High-resolution mapping of physiology and gene expression within an individual coral colony

Asking whether the differences in environmental conditions results in different physiology and gene expression across a colony, we divided a small *S. pistillata* coral colony into 13 branches, recording the position of each branch within the colony (cardinal direction and height ring). We then further sub-divided the branches into locations from deeper inside the colony (base), approximately mid-way up the branch to the location where tips begin to diverge (junction), and toward the outside (two tips per branch) (figure 1b inset). Five branches were analyzed for physiology (e.g., figure 1b) and eight branches were analyzed for gene expression using the additive model in DESeq2, resulting in 32 transcriptome libraries across the three-dimensional space of the coral colony (electronic supplementary material, table S1). The *S. pistillata* colony examined here was genetically homogenous (not chimeric, electronic supplementary material, figure S1), and thus any changes in physiology or gene expression between regions are likely a response of the polyps to their local micro-environmental conditions rather than genotypic differences. The expression of >10,000 of the ~24,000 tested host genes was affected by at least one of the tested factors: location at branch, ring height, and cardinal direction (electronic supplementary material, tables S2, S3). We observed a clear differentiation in host gene expression between branch positions and from the top to the bottom of the colony (figure 1e, figure 2, electronic supplementary material, table S3). In contrast, the effect of the cardinal direction of the colony was far less pronounced (figure 1e). Combined, we observed an interaction effect between factors (electronic supplementary material, tables, S3, S5), as, for

instance, groups of genes involved in signaling pathways important in development that are significantly enriched in branch tips versus bases as compared to up versus down interactions (figure 2b, electronic supplementary material, figure S2). On the other hand, of ~12,000 tested symbiont genes, only ~150 were DE (electronic supplementary material, table S4). The host vs. symbiont differences, shown here, are partly attributed to technical differences in statistical power due to lower symbiont read counts (see also Methods), and likely represent an underestimation of the symbiont differential expression. Comparing colony interior with periphery, host gene expression patterns are more similar between junction and base branch positions compared to tips, although not the same at junctions and bases (figure 1e). Differentiation in gene expression patterns of the photosymbionts is not as clearly delineated as for the host (figure 1f), but nevertheless the expression patterns differ between cardinal directions ($p<0.0007$, ADONIS test, electronic supplementary material, table S8), likely reflecting the different light regimes experienced on different sides of the colony, visible in figure 1a.

(c) Patterns in gene expression are conserved between Stylophora pistillata *and* Acropora *spp.*

A previous study analyzed the differences in gene expression between branch tips and bases in a different coral, *Acropora* spp. [20]. This provided an opportunity to identify conserved intra-colonial patterns in gene expression between these two coral species, which likely diverged at least 200 million years ago [46]. We identified ~9,600 putative orthologous expressed genes between *S. pistillata* and two species of *Acropora* spp. [20], based on reciprocal BLAST. Interestingly, from a total of 952 genes that were DE in *Acropora* spp. along the branch axis, 70% were also DE in *S. pistillata* (672), and 90% of these exhibited the same fold change trend (figure 2a, electronic supplementary material, table S9). The dependence of fold changes and DE

significance between the two species is highly significant (Fisher's exact test, p-value < 2.2e-16). Overall, these results indicate that micro-environmental dependence of gene DE, specifically at tips versus bases, reflects an evolutionarily conserved pattern rather than a species-specific or colony-specific pattern, being observed in members of both robust (here) and complex [20] scleractinian clades.

(d) Gene expression patterns suggest differences in host versus photosymbiont metabolism

We next inferred potential broad-scale changes in cellular and metabolic functions within the host and the symbiont by identifying KEGG and Gene Ontology (GO) enrichment patterns associated with micro-environmental changes, in both the host (figure 2b, electronic supplementary material, tables S10, S11), and the photosymbiont (figure 2c, electronic supplementary material, table S12). As expected, differential expression of broad clusters of host KEGG terms and photosymbiont GO terms (figure 2b, c) mirrors the pattern observed for the differential expression of all genes within the host and symbiont (figure 1e, f), with many more terms exhibiting DE in the coral host along the branch axis compared to the height ring or cardinal axis (figure 2b), and more terms differed along cardinal direction for the photosymbiont (figure 2c).

Most differentially expressed host genes grouped by KEGG term tended to be up-regulated in the tip relative to the junction or base, although genes with KEGG terms associated with protein production, modification, and degradation exhibited quite variable expression (figure 2b, electronic supplementary material, tables S10, S11). Specifically, many terms related to cell metabolism were enriched in the tips versus the bases, including carbohydrate metabolism (e.g., glycolysis and the TCA cycle, oxidative phosphorylation, mitochondrial biosynthesis), amino

acid biosynthesis and metabolism, and lipid metabolism (figure 2a). We further tested which functional groups are enriched with conserved tip vs. base DE gene patterns between the taxa (figure 2a, b). As indicated by green KEGG term text in figure 2b, many fundamental processes such as metabolism show similar DE trends and enrichment between these two genera (electronic supplementary material, tables S9, S10), indicating a conserved response between the taxa. “Zooming in” from the KEGG terms to the underlying genes, we note that genes related to oxidative phosphorylation, such as ATP synthase, cytochrome c oxidase, co-enzyme Q, and NADH dehydrogenase tend to be up-regulated at branch tips across the species. In addition, multiple genes for succinate dehydrogenase as well as other individual genes comprising the citric acid cycle, were also more highly expressed at branch tips than junctions or bases in *S. pistillata* and many of these showed similar regulation patterns in the *Acropora* spp. Finally, most of the >100 differentially expressed genes with KEGG terms for mitochondrial biogenesis are up-regulated at tips compared with junctions and bases in *S. pistillata* and many of their likely homologs are also up-regulated at branch tips in *Acropora* spp.

Intriguingly, the patterns of gene expression observed in the host were not all recapitulated in the photosymbiont. Although some symbiont GO terms associated with photosynthesis were enriched in the tip vs the base in the symbionts (e.g., those involved in light-harvesting and the thylakoid), others were not, including terms involved with carbon fixation (figure 2c). In accordance with the gene expression data, no differing patterns in photophysiology were found along branch axis, measured here as chlorophyll and symbiont density per both total protein and area (electronic supplementary material, tables S7, S13). Indeed, previous studies have shown that the products of photosynthesis can be translocated from the base to the tips in branching

corals [47, 48]. Rather than exhibiting tip-to-base functional differences, many of the terms associated with symbiont photosynthesis (both light and dark reactions) were found to differ along cardinal direction rather than branch axis, being enriched in south-facing branches (figure 2c). This may be due to the direction of the sun. These enrichment patterns are an underestimation due to the limited number of tested photosymbiont genes and DE detection power (see Methods). Furthermore, correlations between mRNA abundance and physiological patterns may not be high due to translation level effects, translocation of host/symbiont products, food particle capture by the host, etc., which may lead to differences in symbiont transcriptional control.

(e) Developmental pathways are differentially expressed along the branch axis

In addition to pathways related to metabolism, several KEGG terms associated with development and morphological plasticity in colony architecture were also differentially expressed between branch tips and junctions or bases. For example, the Wnt signaling pathway was enriched at branch tips versus the bases in both *S. pistillata* (figure 2b) and *Acropora* spp. [20]. This pathway, which transmits information from outside to inside cells, is associated with cell differentiation and axis patterning in cnidarians [e.g., 49, 50 among others] among others, reviewed in [reviewed in 51], as well as in bilaterians such as *Drosophila* [e.g., 52]. Similarly, the TGFβ signaling pathway was also enriched in *S. pistillata* branch tips (figure 2b), although this was not observed in *Acropora* spp. [20]; this pathway has been implicated for a role in development and calcification in corals [53]. At the individual gene level, we observed that fibroblast growth factors, which could aid in development of limbs [reviewed in 54] and in production of nerve cells [reviewed in 55] were significantly up-regulated at branch tips. Half of the genes involved in mitochondrial biosynthesis were also up-regulated at branch tips. Further,

two different bone morphogenetic proteins (BMPs), which may play a role in axial patterning in cnidarian polyps [56] and in budding [57], were up-regulated at branch tips here. Finally, several retinol dehydrogenases are up-regulated at branch tips, where light levels tend to be higher, an observation shared with *Acropora* spp. [20]. These proteins are associated with photoreceptors in higher organisms, although the link to chromophores in non-eye-bearing invertebrates such as corals has not been characterized [58].

In addition to morphological plasticity, gamete production has also been shown to vary along branches axes across several coral taxa with gametogenesis typically occurring preferentially deeper in the colony [59-61]. We observed the highest expression of several testis-specific genes, such as testis-specific chromodomain protein Y 1-like and testis-specific protein kinases at *S. pistillata* branch junctions (electronic supplementary material, table S2). In humans, these genes are associated with chromosome Y [62] and/or may be involved in sperm structure [63]. This is consistent with observations that the highest planulae production in *Pocillopora damicornis* occurs at branch junctions [61]. Interestingly, we observed up-regulation of octopamine receptors at branch tips, suggestive of higher maturation of ovaries and testes in that location [64].

(f) Changes in expression of genes potentially related to predation along branch axis

As described above, many metabolic processes were enriched in the tips versus the bases, whereas there is little evidence for higher photosynthesis by photosymbionts at branch tips. Asking whether this could be due to more heterotrophic food input in the tips (e.g., through predation), we analyzed the tissue toxicity (hemolytic activity) and gene expression patterns of putative toxins. Although there was no difference in nematocyst abundance along branch axes

(figure 3a, electronic supplementary material, table S7), tissue hemolytic activity was highest at branch tips (figure 3b, electronic supplementary material, table S7), consistent with previous studies in *S. pistillata* [65]. Using reciprocal BLAST, we identified 22 putative toxin genes [66], encoding cytolysins, phospholipase A2 toxins, SCRiPs (small cysteine rich peptides) and a potential Kunitz/K channel toxin (electronic supplementary material, table S14). We also compared these genes to the reciprocal BLAST results against the *Acropora* spp. dataset [20], finding only two orthologous matches, a SCRiP and an uncharacterized protein. Like their *S. pistillata* counterparts, they were not differentially expressed between branch tips and bases in any taxa (electronic supplementary material, table S15). In our putative toxin dataset, we observed 13 and 11 DE genes between branch tips and bases or junctions, respectively (figure 3c, d, electronic supplementary material, table S15 and figure S3). Up-regulation of genes encoding potential toxins at branch tips has previously been observed in colonial corals [20, 67]. The two most abundantly expressed putative toxin genes encode for a cytolysin and a second SCRiP, with the rest of the toxin genes having much lower overall expression levels (figure 3c, d; electronic supplementary material, table S15). The cytolysin was more abundantly expressed at the tips, whereas the SCRiP was more abundantly expressed at branch bases (figure 3c, d). The highly expressed cytolysin is of particular interest as it belongs to the actinoporin family, and a hemolytic protein from this family, likely the protein or an isoform of the highly expressed gene here (electronic supplementary material, figure S4), has previously been isolated from *S. pistillata* [65]. Actinoporins are ~20 kDa water-soluble proteins which are lethal when injected into crustaceans [68], and which insert themselves into membranes, particularly those containing sphingomyelins [69]. They have been immunolocalized to tentacle nematocysts as well as to mesenterial filaments [70]. SCRiPs are ~5 kDa peptides which may be anthozoan-specific [71,

72], with evidence that they have neurotoxic effects [72], although their function remains to be fully clarified. Taken together, all data support that branch tips play the predominant role in venom-based competition, defense, and predation.

The higher hemolytic activity and larger number of toxins more abundantly expressed at branch tips suggest that the tips play the dominant role in venom-based competition, defense, and predation, although more work is needed to identify the role of putative toxins such as SCRiPs, which are more abundantly expressed at branch bases, and the potential contribution and roles of photosymbiont toxin production [73, 74]. While it is difficult to disentangle toxin effects on competition and defense from predation, based on higher flow at the edges of colonies [11], colonies' edges are likely exposed to higher food loads than are colony interiors. We therefore queried genes related to digestion and observed that many peptidases were differentially expressed, but not in a clear pattern along the branches with approximately half up-regulated at the tips. Similarly, multiple lipases were differentially expressed between branch locations, but no general trend was observed. However, pancreatic lipase expression, which has been observed in gastric cirri in a scyphozoan [75], was found to be significantly up-regulated to a high degree at branch tips compared to junctions and bases here. We also observed up-regulation of three chitinases in branch tips versus bases, which could support extracellular digestion of arthropod prey [75]. In contrast, an amylase which converts starch and glycogen - biomolecules used by the photosymbiont and host, respectively, to store photosynthates [76] - into simple sugars, was down-regulated at the tips versus junctions and bases. Thus, while our results suggest differences along the branch axis of functions related to pry capture and defense, including both toxicity and

digestion, further work is needed to fully characterize to what extent different parts of the corals obtain their nutrition from different sources (predation versus the photosymbionts).

(g) Changes in expression of known biomineralization genes along branch axis

Shallow water stony corals are most notable for their production of massive reef structures, growing in size by adding mineral and new polyps at the tips. We therefore examined in depth skeletal morphological patterns and related gene expression across the three branch locations. Unlike most other physiological parameters across the colony which were not significantly different between branch positions (electronic supplementary material, tables S7, S13), those linked to differences in biomineralization were significantly different between tip versus junction and base locations. Qualitatively, coenosteal spines appear narrowest and thinnest at the tip while base spines exhibit a more distinct microtuberculate texture in their lower portions (figure 4aii, iv, and vi). Such microtuberculate texture with better differentiation of mineral fiber bundles may suggest higher organic matrix content which separates the mineral phase packages to a greater extent [77, 78]. Corallites were closer together and more elliptically shaped at the tip than at the branch junction or base (figure 4b and c; electronic supplementary material, tables S7, S13). Comparable trending toward ellipticity at the tips has been reported in other Pocilloporids [79]. Further, genetically identical *S. pistillata* branches have been shown to have more distantly spaced corallites with thicker theca and longer septa when grown under light spectra biased toward blue wavelengths [80]. Such a spectral shift along a single branch, due to absorbance of red light by water, has been observed in *S. pistillata* tissue at the colony level on the sides versus at the top of ~30 cm diameter colonies [81] and at the branch level along *Acropora millepora* branches toward the colony interior [82]. Growth patterns can also be influenced by flow-

induced effects on calcification, with more branches per area but less sub-branching observed in pocilloporids grown under high versus low flow conditions [83].

We next examined differential expression of known biomineralization-related genes including those for proteins sequenced from *S. pistillata* skeleton and likely directly involved in the calcification mechanism [77, 84-88], as well as a bicarbonate anion transporter observed predominantly in the calicoblastic cell layer and proposed to be indirectly involved in calcification [89] (figure 4e, e; electronic supplementary material, table S16, figure S5). We did not include genes for known skeletal proteins from *Acropora millepora* and *A. digitifera* [90, 91], as not all orthologs have been found in *S. pistillata* skeleton although they exist in the genome, or non-orthologous proteins within the same functional group occur in *S. pistillata* skeleton [92]. Similar to the global gene expression pattern for the host, we observed an up-regulation of biomineralization genes biased toward the tip, with minimal differential expression from the top of the colony (up) to the bottom (down) (figure 4d, e; electronic supplementary material, table S16). Of the 36 biomineralization-related genes that were DE between branch tips and bases, eight orthologous genes were also DE and in the same direction in *Acropora* spp. [20] (electronic supplementary information, table S17). In *S. pistillata*, the bicarbonate anion transporter SLCγ4, a coadhesin-like protein, USOMP8 and a hypothetical protein are strongly up-regulated at branch tips relative to the junctions and bases but are expressed in only low amounts. In contrast, a ZP-domain containing protein, carbonic anhydrase (STPCA2), mammalian ependymin-related protein, and CARP3 are moderately up-regulated at branch tips versus junctions and bases and are very highly expressed overall. These proteins exhibit very different functions with SLCγ4 and STPCA2 involved in regulating carbonate chemistry within

the calcifying space [89, 93], while CARP3, which is a highly acidic protein (35% Asp, 15%Glu [94]) can direct mineralogy toward formation of Mg-calcite and vaterite [95, 96]. CARP3 is up-regulated in newly-settled coral polyps [97, 98], in colonies growing at shallow depths [99], and in coral cell cultures reared at increased pCO_2 [100]. USOMP8 has been sequenced from skeletons of two stony coral species to date [85, 86, 90], and although its function is not known, it is structurally similar to a bone morphogenetic protein inhibitor [86]. Of the remaining known highly acidic coral skeleton genes, CARPs 1 and 4 are up-regulated at branch tips and are moderately expressed; both of these proteins are biased toward Asp residues [94] and are likely involved in nucleation initiation in early mineralization zones of growing septa [77, 101]. In contrast, CARP2 exhibits very low although significantly up-regulated expression at branch tips and is the sole CARP described to date strongly biased toward Glu rather than Asp content [94]. While this protein is suggested to have a role in skeleton extension based on its localization to more soluble growth areas [77], its down-regulation upon settlement in pocilloporid larvae [97, 98], association with ACC phases pre-settlement [97], and low overall expression in the present study may instead point to a role in inhibiting aragonite nucleation. Taking together the existing data and our new cross-colony analysis provides further genetic support for high biomineralization activity of branch tips in contrast to junctions and bases [e.g., 102]. Energy for higher calcification rates at branch tips could come from two sources. First, there is evidence of translocation of ATP from tissue regions deeper in the colony with relatively high photosynthetic rates [103] to branch tips. Secondly, our and previous data suggest that the potential for predation is higher at branch tips, with higher toxin gene expression and hemolytic activity at that location (figure 3) [20, 65]. This further suggests that biomineralization gene expression and

skeleton morphology patterns observed at the sub-polyp scale (i.e., centers of calcification in growing tips of septa) are recapitulated at the branch scale [99].

Unlike the genes up-regulated at branch tips for which functions of many have been elucidated to some extent, all biomineralization genes down-regulated at branch tips remain to be functionally well-characterized in corals and all but one, annotated as ‘deleted in malignant brain tumors 1-like’, exhibit very low expression overall.

4 Summary and Conclusions

Some colonial cnidarians, particularly hydrozoans, exhibit a clear division of labor inside the colony, with functionally and morphologically distinct polyps across the colony [104]. While no obvious division of labor at the polyp scale is observed in corals, our results show, from molecular to physiological and morphological scales, a functional specialization by clusters of polyps due to their locations on coral branches likely related to the microenvironments they encounter [105] (figure 5). In simplest terms, polyps at the tips are more exposed to light and water flow, and their skeletons are likely extending at a faster rate, than are those found lower in the branches. Branch tips are also sites of higher potential for envenomation for colony defense and predation, as well as possibly for enhanced prey capture. These plastic responses by genetically identical polyps can then be communicated through the coenosarc to the rest of the colony to allow for enhanced resource sharing [106-108]. Such plasticity may aid in colony recovery after partial mortality events, such as those due to bleaching [109], and may be integral to adaptation to environmental change [110]. Further, the expression patterns underlying the

tested micro-environmental differences are found to be evolutionary conserved in the distantly-related stony corals *S. pistillata* and *Acropora* spp.

5 Electronic Supplementary Material Availability, Tables

All electronic supplementary tables are available on the Dryad data repository under the dataset https://doi.org/10.5061/dryad.tht76hdzc.

6 Funding

This study was supported by grants 1239/13 and 312/15 from the Israel Science Foundation (to DS and TM, respectively) and by the associated grant number 2236/16 from the Israeli National Center for Personalized Medicine (to DS). This project has received funding to TM from the European Research Council (ERC) under the European Union's Horizon 2020 research and innovation programme (grant agreement No 755876). JLD was supported by the Zuckerman STEM Leadership Program. We thank the Crown Genomics Institute of the Nancy and Stephen Grand Israel National Center for Personalized Medicine, Weizmann Institute of Science for transcriptome sequencing. Computations presented in this work were performed on the Hive computer cluster at the University of Haifa, which is partly funded by ISF grant 2155/15.

7 Acknowledgements

We thank Yarden Ben-Tabou de-Leon for drawing the summary figure 5 and Dikla Aharonovich for guidance and laboratory assistance.

8 Author Contributions

YP, OY, DT, DS, and TM designed the study. YP, OY, ES prepared the samples. JLD, AM, YP, OY, ES, and JS analyzed the data. All authors wrote the manuscript and approve of this submission.

9 References

1. Spalding M., Grenfell A. 1997 New estimates of global and regional coral reef areas. *Coral Reefs* **16**(4), 225-230.
2. Hoegh-Guldberg O., Jacob D., Taylor M., Bolaños T.G., Bindi M., Brown S., Camilloni I., Diedhiou A., Djalante R., Ebi K. 2019 The human imperative of stabilizing global climate change at 1.5° C. *Science* **365**(6459), eaaw6974.
3. Hughes T.P. 1994 Catastrophes, phase shifts, and large-scale degradation of a Caribbean coral reef. *Science* **265**(5178), 1547-1551.
4. Graham N.A., Wilson S.K., Jennings S., Polunin N.V., Bijoux J.P., Robinson J. 2006 Dynamic fragility of oceanic coral reef ecosystems. *Proceedings of the National Academy of Sciences* **103**(22), 8425-8429.
5. Bellwood D.R., Hughes T.P., Folke C., Nyström M. 2004 Confronting the coral reef crisis. *Nature* **429**(6994), 827-833.
6. Falkowski P.G., Dubinsky Z., Muscatine L., Porter J.W. 1984 Light and the bioenergetics of a symbiotic coral. *Bioscience* **34**(11), 705-709.
7. Grover R., Maguer J.-F., Allemand D., Ferrier-Pages C. 2008 Uptake of dissolved free amino acids by the scleractinian coral *Stylophora pistillata*. *The Journal of Experimental Biology* **211**, 860-865.

8. Martinez S., Kolodny Y., Shemesh E., Scucchia F., Nevo R., Levin-Zaidman S., Paltiel Y., Keren N., Tchernov D., Mass T. 2020 Energy sources of the depth-generalist mixotrophic coral *Stylophora pistillata*. *Frontiers in Marine Science* **7**, 988.
9. Houlbrèque F., Ferrier-Pagès C. 2009 Heterotrophy in tropical scleractinian corals. *Biological Reviews* **84**(1), 1-17. (doi:10.1111/j.1469-185X.2008.00058.x).
10. Schmidt C.A., Daly N.L., Wilson D.T. 2019 Coral venom toxins. *Frontiers in Ecology and Evolution* **7**, 320.
11. Chang S., Elkins C., Alley M., Eaton J., Monismitha S. 2009 Flow inside a coral colony measured using magnetic resonance velocimetry. *Limnol Oceanogr* **54**(5), 1819-1827.
12. Carpenter L.W., Patterson M.R. 2007 Water flow influences the distribution of photosynthetic efficiency within colonies of the scleractinian coral *Montastrea annularis* (Ellis and Solander, 1786); implications for coral bleaching. *J Exp Mar Biol Ecol* **351**(1-2), 10-26.
13. Sebens K.P., Witting J., Helmuth B. 1997 Effects of water flow and branch spacing on particle capture by the reef coral *Madracis mirabilis* (Duchassaing and Michelotti). *J Exp Mar Biol Ecol* **211**(1), 1-28.
14. Mass T., Brickner I., Hendy E., Genin A. 2011 Enduring physiological and reproductive benefits of enhanced flow for a stony coral. *Limnol Oceanogr* **56**(6), 2176-2188.
15. Mass T., Einbinder S., Brokovich E., Shashar N., Vago R., Erez J., Dubinsky Z. 2007 Photoacclimation of *Stylophora pistillata* to light extremes: metabolism and calcification. *Mar Ecol Prog Ser* **334**, 93-102.
16. Dennison W.C., Barnes D.J. 1988 Effect of water motion on coral photosynthesis and calcification. *J Exp Mar Biol Ecol* **115**(1), 67-77.
17. Mass T., Genin A., Shavit U., Grinstein M., Tchernov D. 2010 Flow enhances photosynthesis in marine benthic autotrophs by increasing the efflux of oxygen from the organism to the water. *Proceedings of the National Academy of Sciences* **107**(6), 2527-2531.
18. Anthony K.R., Hoogenboom M.O., Connolly S.R. 2005 Adaptive variation in coral geometry and the optimization of internal colony light climates. *Funct Ecol* **19**(1), 17-26.
19. Ralph P., Gademann R., Larkum A., Kühl M. 2002 Spatial heterogeneity in active chlorophyll fluorescence and PSII activity of coral tissues. *Mar Biol* **141**(4), 639-646.
20. Hemond E.M., Kaluziak S.T., Vollmer S.V. 2014 The genetics of colony form and function in Caribbean *Acropora* corals. *BMC Genomics* **15**(1), 1133.
21. Ritchie R. 2008 Universal chlorophyll equations for estimating chlorophylls a, b, c, and d and total chlorophylls in natural assemblages of photosynthetic organisms using acetone, methanol, or ethanol solvents. *Photosynthetica* **46**(1), 115-126.
22. Primor N., Zlotkin E. 1975 On the ichthyotoxic and hemolytic action of the skin secretion of the flatfish *Pardachirus marmoratus* (Soleidae). *Toxicon* **13**(4), 227-231.
23. Bartosz G., Finkelshtein A., Przygodzki T., Bsor T., Nesher N., Sher D., Zlotkin E. 2008 A pharmacological solution for a conspecific conflict: ROS-mediated territorial aggression in sea anemones. *Toxicon* **51**(6), 1038-1050.
24. Marsh Jr J.A. 1970 Primary productivity of reef□building calcareous red algae. *Ecology* **51**(2), 255-263.
25. LaJeunesse T.C., Parkinson J.E., Gabrielson P.W., Jeong H.J., Reimer J.D., Voolstra C.R., Santos S.R. 2018 Systematic revision of Symbiodiniaceae highlights the antiquity and diversity of coral endosymbionts. *Curr Biol* **28**(16), 2570-2580. e2576.
26. Buchfink B., Xie C., Huson D.H. 2015 Fast and sensitive protein alignment using DIAMOND. *Nat Methods* **12**(1), 59-60.

27. Dobin A., Davis C.A., Schlesinger F., Drenkow J., Zaleski C., Jha S., Batut P., Chaisson M., Gingeras T.R. 2013 STAR: ultrafast universal RNA-seq aligner. *Bioinformatics* **29**(1), 15-21.
28. Voolstra C.R., Li Y., Liew Y.J., Baumgarten S., Zoccola D., Flot J.-F., Tambutté S., Allemand D., Aranda M. 2017 Comparative analysis of the genomes of *Stylophora pistillata* and *Acropora digitifera* provides evidence for extensive differences between species of corals. *Scientific Reports* **7**(1), 17583.
29. Aranda M., Li Y., Liew Y.J., Baumgarten S., Simakov O., Wilson M.C., Piel J., Ashoor H., Bougouffa S., Bajic V.B. 2016 Genomes of coral dinoflagellate symbionts highlight evolutionary adaptations conducive to a symbiotic lifestyle. *Scientific Reports* **6**(1), 1-15.
30. Love M.I., Huber W., Anders S. 2014 Moderated estimation of fold change and dispersion for RNA-seq data with DESeq2. *Genome Biology* **15**(12), 1-21.
31. DePristo M.A., Banks E., Poplin R., Garimella K.V., Maguire J.R., Hartl C., Philippakis A.A., Del Angel G., Rivas M.A., Hanna M. 2011 A framework for variation discovery and genotyping using next-generation DNA sequencing data. *Nat Genet* **43**(5), 491.
32. Bryant D.M., Johnson K., DiTommaso T., Tickle T., Couger M.B., Payzin-Dogru D., Lee T.J., Leigh N.D., Kuo T.-H., Davis F.G. 2017 A tissue-mapped axolotl de novo transcriptome enables identification of limb regeneration factors. *Cell Reports* **18**(3), 762-776.
33. Young M.D., Wakefield M.J., Smyth G.K., Oshlack A. 2012 goseq: Gene Ontology testing for RNA-seq datasets. *R Bioconductor* **8**, 1-25.
34. Sergushichev A.A. 2016 An algorithm for fast preranked gene set enrichment analysis using cumulative statistic calculation. *BioRxiv*, 060012.
35. Subramanian A., Tamayo P., Mootha V.K., Mukherjee S., Ebert B.L., Gillette M.A., Paulovich A., Pomeroy S.L., Golub T.R., Lander E.S. 2005 Gene set enrichment analysis: a knowledge-based approach for interpreting genome-wide expression profiles. *Proceedings of the National Academy of Sciences* **102**(43), 15545-15550.
36. Yu G., Lam T.T.-Y., Zhu H., Guan Y. 2018 Two methods for mapping and visualizing associated data on phylogeny using ggtree. *Mol Biol Evol* **35**(12), 3041-3043.
37. Team R. 2019 RStudio: Integrated Development for R. (Boston, MA, RStudio, Inc.
38. Hossain M.M., Staples A.E. 2020 Mass transport and turbulent statistics within two branching coral colonies. *Fluids* **5**(3), 153.
39. Schiller C., Herndl G.J. 1989 Evidence of enhanced microbial activity in the interstitial space of branched corals: possible implications for coral metabolism. *Coral Reefs* **7**(4), 179-184.
40. Garren M., Son K., Raina J.-B., Rusconi R., Menolascina F., Shapiro O.H., Tout J., Bourne D.G., Seymour J.R., Stocker R. 2014 A bacterial pathogen uses dimethylsulfoniopropionate as a cue to target heat-stressed corals. *The ISME Journal* **8**(5), 999-1007.
41. Bak R.P.M., Joenje M., Jong I.d., Lambrechts D.Y.M., Nieuwland G. 1998 Bacterial suspension feeding by coral reef benthic organisms. *Mar Ecol Prog Ser* **175**, 285-288. (doi:10.3354/meps175285).
42. Ritchie K.B. 2006 Regulation of microbial populations by coral surface mucus and mucus-associated bacteria. *Mar Ecol Prog Ser* **322**, 1-14.
43. Nakajima R., Yoshida T., Azman B.A.R., Zaleha K., Othman B.H.R., Toda T. 2009 In situ release of coral mucus by *Acropora* and its influence on the heterotrophic bacteria. *Aquat Ecol* **43**(4), 815-823.

44. Gibbin E., Gavish A., Domart-Coulon I., Kramarsky-Winter E., Shapiro O., Meibom A., Vardi A. 2018 Using NanoSIMS coupled with microfluidics to visualize the early stages of coral infection by *Vibrio coralliilyticus*. *BMC Microbiol* **18**(1), 1-10.
45. Winkler R., Antonius A., Abigail Renegar D. 2004 The skeleton eroding band disease on coral reefs of Aqaba, Red Sea. *Mar Ecol* **25**(2), 129-144.
46. Park E., Hwang D.-S., Lee J.-S., Song J.-I., Seo T.-K., Won Y.-J. 2012 Estimation of divergence times in cnidarian evolution based on mitochondrial protein-coding genes and the fossil record. *Mol Phylogen Evol* **62**(1), 329-345.
47. Rinkevich B., Loya Y. 1983 Oriented translocation of energy in grafted reef corals. *Coral Reefs* **1**(4), 243-247.
48. Pearse V.B., Muscatine L. 1971 Role of symbiotic algae (zooxanthallae) in coral calcification. *Biological Bulletin* **141**, 350-363.
49. Duffy D.J., Plickert G., Kuenzel T., Tilmann W., Frank U. 2010 Wnt signaling promotes oral but suppresses aboral structures in *Hydractinia* metamorphosis and regeneration. *Development* **137**(18), 3057-3066.
50. Trevino M., Stefanik D.J., Rodriguez R., Harmon S., Burton P.M. 2011 Induction of canonical Wnt signaling by alsterpaullone is sufficient for oral tissue fate during regeneration and embryogenesis in *Nematostella vectensis*. *Dev Dyn* **240**(12), 2673-2679.
51. Lee P.N., Pang K., Matus D.Q., Martindale M.Q. 2006 A WNT of things to come: evolution of Wnt signaling and polarity in cnidarians. *Semin Cell Dev Biol* **17**(2), 157-167. (doi:http://dx.doi.org/10.1016/j.semcdb.2006.05.002).
52. Siegfried E., Perrimon N. 1994 *Drosophila* wingless: a paradigm for the function and mechanism of Wnt signaling. *Bioessays* **16**(6), 395-404.
53. Gutner-Hoch E., Ben-Asher H.W., Yam R., Shemesh A., Levy O. 2017 Identifying genes and regulatory pathways associated with the scleractinian coral calcification process. *PeerJ* **5**, e3590.
54. Xu X., Weinstein M., Li C., Deng C.-X. 1999 Fibroblast growth factor receptors (FGFRs) and their roles in limb development. *Cell Tissue Res* **296**(1), 33-43.
55. Guillemot F., Zimmer C. 2011 From cradle to grave: the multiple roles of fibroblast growth factors in neural development. *Neuron* **71**(4), 574-588.
56. Reinhardt B., Broun M., Blitz I.L., Bode H.R. 2004 HyBMP5-8b, a BMP5-8 orthologue, acts during axial patterning and tentacle formation in *Hydra*. *Dev Biol* **267**(1), 43-59.
57. Surekha K.L., Khade S., Trimbake D., Patwardhan R., Nadimpalli S.K., Ghaskadbi S. 2020 Differential expression of BMP inhibitors gremlin and noggin in *Hydra* suggests distinct roles during budding and patterning of tentacles. *Dev Dyn*.
58. Albalat R. 2012 Evolution of the genetic machinery of the visual cycle: a novelty of the vertebrate eye? *Mol Biol Evol* **29**(5), 1461-1469.
59. Chornesky E.A., Peters E.C. 1987 Sexual reproduction and colony growth in the scleractinian coral *Porites astreoides*. *Biological Bulletin* **172**(2), 161-177.
60. Oliver J.K. 1987 Aspects of skeletal growth in the Indo-Pacific staghorn coral *Acropora formosa*, James Cook University.
61. Stimson J. 1978 Mode and timing of reproduction in some common hermatypic corals of Hawaii and Enewetak. *Mar Biol* **48**(2), 173-184.
62. Lahn B.T., Page D.C. 1999 Retroposition of autosomal mRNA yielded testis-specific gene family on human Y chromosome. *Nat Genet* **21**(4), 429-433.

63. Walden P.D., Cowan N.J. 1993 A novel 205-kilodalton testis-specific serine/threonine protein kinase associated with microtubules of the spermatid manchette. *Mol Cell Biol* **13**(12), 7625-7635.
64. Chiu Y.-L., Shikina S., Yoshioka Y., Shinzato C., Chang C.-F. 2020 De novo transcriptome assembly from the gonads of a scleractinian coral, *Euphyllia ancora*: molecular mechanisms underlying scleractinian gametogenesis. *BMC Genomics* **21**(1), 1-20.
65. Ben-Ari H., Paz M., Sher D. 2018 The chemical armament of reef-building corals: inter- and intra-specific variation and the identification of an unusual actinoporin in *Stylophora pistilata*. *Scientific Reports* **8**(1), 1-13.
66. Rachamim T., Morgenstern D., Aharonovich D., Brekhman V., Lotan T., Sher D. 2015 The dynamically evolving nematocyst content of an anthozoan, a scyphozoan, and a hydrozoan. *Mol Biol Evol* **32**(3), 740-753.
67. Hemond E.M., Vollmer S.V. 2015 Diurnal and nocturnal transcriptomic variation in the Caribbean staghorn coral, *Acropora cervicornis*. *Mol Ecol* **24**(17), 4460-4473.
68. Giese C., Mebs D., Werding B. 1996 Resistance and vulnerability of crustaceans to cytolytic sea anemone toxins. *Toxicon* **34**(8), 955-958.
69. Alvarez C., Mancheno J.M., Martínez D., Tejuca M., Pazos F., Lanio M.E. 2009 Sticholysins, two pore-forming toxins produced by the Caribbean Sea anemone *Stichodactyla helianthus*: their interaction with membranes. *Toxicon* **54**(8), 1135-1147.
70. Basulto A., Pérez V.M., Noa Y., Varela C., Otero A.J., Pico M.C. 2006 Immunohistochemical targeting of sea anemone cytolysins on tentacles, mesenteric filaments and isolated nematocysts of *Stichodactyla helianthus*. *Journal of Experimental Zoology Part A: Comparative Experimental Biology* **305**(3), 253-258.
71. Sunagawa S., DeSalvo M.K., Voolstra C.R., Reyes-Bermudez A., Medina M. 2009 Identification and gene expression analysis of a taxonomically restricted cysteine-rich protein family in reef-building corals. *PLoS ONE* **4**(3), e4865.
72. Jouiaei M., Sunagar K., Federman Gross A., Scheib H., Alewood P.F., Moran Y., Fry B.G. 2015 Evolution of an ancient venom: recognition of a novel family of cnidarian toxins and the common evolutionary origin of sodium and potassium neurotoxins in sea anemone. *Mol Biol Evol* **32**(6), 1598-1610.
73. Nakamura H., Asari T., Ohizumi Y., Kobayashi J.i., Yamasu T., Murai A. 1993 Isolation of zooxanthellatoxins, novel vasoconstrictive substances from the zooxanthella *Symbiodinium* sp. *Toxicon* **31**(4), 371-376.
74. Beedessee G., Hisata K., Roy M.C., Satoh N., Shoguchi E. 2015 Multifunctional polyketide synthase genes identified by genomic survey of the symbiotic dinoflagellate, *Symbiodinium minutum*. *BMC Genomics* **16**(1), 1-11.
75. Steinmetz P.R. 2019 A non-bilaterian perspective on the development and evolution of animal digestive systems. *Cell Tissue Res* **377**(3), 321-339.
76. Kopp C., Domart-Coulon I., Escrig S., Humbel B.M., Hignette M., Meibom A. 2015 Subcellular investigation of photosynthesis-driven carbon assimilation in the symbiotic reef coral *Pocillopora damicornis*. *MBio* **6**(1).
77. Mass T., Drake J.L., Peters E.C., Jiang W., Falkowski P.G. 2014 Immunolocalization of skeletal matrix proteins in tissue and mineral of the coral *Stylophora pistillata*. *Proceedings of the National Academy of Sciences* **111**(35), 12728-12733.
78. Coronado I., Fine M., Bosellini F.R., Stolarski J. 2019 Impact of ocean acidification on crystallographic vital effect of the coral skeleton. *Nature Communications* **10**(1), 1-9.

79. Schmidt-Roach S., Miller K.J., Lundgren P., Andreakis N. 2014 With eyes wide open: a revision of species within and closely related to the *Pocillopora damicornis* species complex (Scleractinia; Pocilloporidae) using morphology and genetics. *Zool J Linn Soc* **170**(1), 1-33.
80. Rocha R.J., Silva A.M., Fernandes M.H.V., Cruz I.C., Rosa R., Calado R. 2014 Contrasting light spectra constrain the macro and microstructures of scleractinian corals. *PloS One* **9**(8).
81. Kaniewska P., Magnusson S.H., Anthony K.R., Reef R., Kühl M., Hoegh□Guldberg O. 2011 Importance of macro- versus microstructure in modulating light levels inside coral colonies. *J Phycol* **47**(4), 846-860.
82. Wangpraseurt D., Polerecky L., Larkum A.W., Ralph P.J., Nielsen D.A., Pernice M., Kühl M. 2014 The in situ light microenvironment of corals. *Limnol Oceanogr* **59**(3), 917-926.
83. Paz-García D.A., Aldana-Moreno A., Cabral-Tena R.A., García-De-León F.J., Hellberg M.E., Balart E.F. 2015 Morphological variation and different branch modularity across contrasting flow conditions in dominant *Pocillopora* reef-building corals. *Oecologia* **178**(1), 207-218.
84. Puverel S., Tambutté E., Pereira-Mouries L., Zoccola D., Allemand D., Tambutté S. 2005 Soluble organic matrix of two Scleractinian corals: Partial and comparative analysis. *Comparative Biochemistry and Physiology Part B* **141**, 480-487.
85. Peled Y., Drake J.L., Malik A., Almuly R., Lalzar M., Morgenstern D., Mass T. 2020 Optimization of skeletal protein preparation for LC–MS/MS sequencing yields additional coral skeletal proteins in *Stylophora pistillata*. *BMC Materials* **2**(1), 8. (doi:10.1186/s42833-020-00014-x).
86. Drake J.L., Mass T., Haramaty L., Zelzion E., Bhattacharya D., Falkowski P.G. 2013 Proteomic analysis of skeletal organic matrix from the stony coral *Stylophora pistillata*. *Proceedings of the National Academy of Sciences* **110**(10), 3788-3793.
87. Mummadisetti M.P., Drake J.L., Falkowski P.G. accepted The spatial network of skeletal proteins in a stony coral. *Journal of The Royal Society Interface*.
88. Bertucci A., Tambutté S., Supuran C., Allemand D., Zoccola D. 2011 A new coral carbonic anhydrase in *Stylophora pistillata*. *Mar Biotechnol* **13**(5), 992-1002. (doi:10.1007/s10126-011-9363-x).
89. Zoccola D., Ganot P., Bertucci A., Caminiti-Segonds N., Techer N., Voolstra C.R., Aranda M., Tambutté E., Allemand D., Casey J.R. 2015 Bicarbonate transporters in corals point towards a key step in the evolution of cnidarian calcification. *Scientific Reports* **5**.
90. Ramos-Silva P., Kaandorp J., Huisman L., Marie B., Zanella-Cleon I., Guichard N., Miller D.J., Marin F. 2013 The skeletal proteome of the coral *Acropora millepora*: The evolution of calcification by cooption and domain shuffling. *Mol Biol Evol*. (doi:10.1093/molbev/mst109).
91. Takeuchi T., Yamada L., Shinzato C., Sawada H., Satoh N. 2016 Stepwise evolution of coral biomineralization revealed with genome-wide proteomics and transcriptomics. *PLoS One* **11**(6), e0156424. (doi:10.1371/journal.pone.0156424).
92. Zaquin T., Malik A., Drake J.L., Putnam H.M., Mass T. accepted Evolution of protein-mediated biomineralization in scleractinian corals. *Frontiers in Genetics*.
93. Zoccola D., Innocenti A., Bertucci A., Tambutté E., Supuran C.T., Tambutté S. 2016 Coral carbonic anhydrases: regulation by ocean acidification. *Mar Drugs* **14**(6), 109.
94. Mass T., Drake Jeana L., Haramaty L., Kim J.D., Zelzion E., Bhattacharya D., Falkowski Paul G. 2013 Cloning and characterization of four novel coral acid-rich proteins that precipitate

carbonates in vitro. *Curr Biol* **23**(12), 1126-1131. (doi:http://dx.doi.org/10.1016/j.cub.2013.05.007).

95. Gavriel R., Nadav□Tsubery M., Glick Y., Yarmolenko A., Kofman R., Keinan□Adamsky K., Berman A., Mass T., Goobes G. 2018 The coral protein CARP3 acts from a disordered mineral surface film to divert aragonite crystallization in favor of Mg□calcite. *Advanced Functional Materials* **28**(21), 1707321.

96. Laipnik R.a., Bissi V., Sun C.-Y., Falini G., Gilbert P.U., Mass T. 2020 Coral acid rich protein selects vaterite polymorph in vitro. *Journal of Structural Biology* **209**(2), 107431.

97. Akiva A., Neder M., Kahil K., Gavriel R., Pinkas I., Goobes G., Mass T. 2018 Minerals in the pre-settled coral *Stylophora pistillata* crystallize via protein and ion changes. *Nature Communications* **9**(1), 1880.

98. Mass T., Putnam H.M., Drake J.L., Zelzion E., Gates R.D., Bhattacharya D., Falkowski P.G. 2016 Temporal and spatial expression patterns of biomineralization proteins during early development in the stony coral *Pocillopora damicornis*. *Proceedings of the Royal Society B: Biological Sciences* **283**(1829), 20160322.

99. Malik A., Einbinder S., Martinez S., Tchernov D., Haviv S., Almuly R., Zaslansky P., Polishchuk I., Pokroy B., Stolarski J. 2021 Molecular and skeletal fingerprints of scleractinian coral biomineralization: from the sea surface to mesophotic depths. *Acta Biomater* **120**, 263-276.

100. Drake J.L., Schaller M.F., Mass T., Godfrey L., Fu A., Sherrell R.M., Rosenthal Y., Falkowski P.G. 2017 Molecular and geochemical perspectives on the influence of CO_2 on calcification in coral cell cultures. *Limnol Oceanogr*.

101. Mass T., Drake J.L., Heddleston J.M., Falkowski P.G. 2017 Nanoscale visualization of biomineral formation in coral proto-polyps. *Curr Biol* **27**(20), 3191-3196. e3193.

102. Goreau T.F. 1959 The physiology of skeleton formation in corals. I. A method for measuring the rate of calcium deposition by corals under different conditions. *Biological Bulletin* **116**, 59-75. (doi:10.2307/1539156).

103. Fang L.-S., Chen Y.-w.J., Chen C.-S. 1989 Why does the white tip of stony coral grow so fast without zooxanthellae? *Mar Biol* **103**(3), 359-363.

104. Cartwright P., Bowsher J., Buss L.W. 1999 Expression of a Hox gene, Cnox-2, and the division of labor in a colonial hydroid. *Proceedings of the National Academy of Sciences* **96**(5), 2183-2186.

105. Rueffler C., Hermisson J., Wagner G.P. 2012 Evolution of functional specialization and division of labor. *Proceedings of the National Academy of Sciences* **109**(6), E326-E335.

106. Mackie G. 1986 From aggregates to integrates: physiological aspects of modularity in colonial animals. *Philosophical Transactions of the Royal Society of London B, Biological Sciences* **313**(1159), 175-196.

107. Rosen B. 1986 Modular growth and form of corals: a matter of metamers? *Philosophical Transactions of the Royal Society of London B, Biological Sciences* **313**(1159), 115-142.

108. Ryland J., Warner G. 1986 Growth and form in modular animals: ideas on the size and arrangement of zooids. *Philosophical Transactions of the Royal Society of London B, Biological Sciences* **313**(1159), 53-76.

109. Matsuda S.B., Huffmyer A.S., Lenz E.A., Davidson J.M., Hancock J.R., Przybylowski A., Innis T., Gates R.D., Barott K.L. 2020 Coral bleaching susceptibility Is predictive of subsequent mortality sithin but not between coral species. *Frontiers in Ecology and Evolution* **8**(178). (doi:10.3389/fevo.2020.00178).

110. Kenkel C.D., Matz M.V. 2016 Gene expression plasticity as a mechanism of coral adaptation to a variable environment. *Nature Ecology & Evolution* **1**(1), 1-6.

9 Figure Legends

Figure 1. Micro-environments and responses in sections of individual coral colonies. The *S. pistillata* colony analyzed for physiological and transcriptomic differences across the colony (a); with branches that were analyzed for physiological parameters noted on opposite sides of a three-dimensional model of the colony (b). Inset in (b) shows branch axis sampling locations at tips (salmon), junction (green), and base (blue). In-situ water column concentrations of dissolved oxygen (c) and total microbial cells (d) between branches inside and outside five colonies of *S. pistillata*. Non-metric multidimensional scaling (NMDS) based on $\log_{10}$FPM of all expressed genes of the coral host (e) and photosymbiont (f). In the host NMDS (e), the ring and branch axis factors are color- and shape-coded, respectively. In the symbiont NMDS (f), the cardinal direction and branch axis factors are color- and shape-coded, respectively. The samples are significantly clustered by these factors (electronic supplementary material, table S5), where ring and branch position clusters are marked by dashed and solid ellipses, respectively.

Figure 2. Venn diagram (a) representing the proportional counts of shared tip vs. base DE genes in *S. pistillata* (here) and two species of *Acropora* [20] (electronic supplementary material, table S9); shaded regions represent genes showing the same DE patterns, where “up” and “down” denote up- and down-regulated. Enrichment patterns of clustered *S. pistillata* KEGG terms (host; b) and photosymbiont GO terms (UniProt *S. microadriaticum*; c) across branch axis, colony height ring, and cardinal direction (host; b) and cardinal direction and branch position (photosymbiont; c) comparisons. Hierarchical tree clustering reflects functional similarity between terms. Color-coded heatmap scores equal to $\log_{10}$(adjusted p-value) of enriched terms multiplied by 1 and -1 for up- and down-regulated genes, respectively (for clarity, values <-2 and >2 are shown as 2 and -2). In the *S. pistillata* terms tree (b), terms enriched in both *S. pistillata* (here) and two species of *Acropora* [20] for tip vs base comparisons, are shown as green labels.

Figure 3. Nematocyst potential. Nematocyst abundance (a) and hemolytic units per area (b), and gene expression patterns of putative toxins as $\log_2$FC between branch tips (positive values) and bases (negative values) (c), and $\log_{10}$FPKM along the branch axis (d). Only significantly DE toxin genes are shown ($p<0.05$). The two most abundant transcripts, a cytolysin annotated as stichotoxin and an uncharacterized gene, for which reciprocal BLAST hits suggest it is a SCRiP (electronic supplementary material, table S14), are noted with a red star (d).

Figure 4. Biomineralization differences between branch locations. Tip corallites exhibited microstructural differences of coenosteal spines compared to junction and base corallites (a; tip in i, ii; junction in iii, iv; base in v, vi). Additionally, corallites at tips were more closely spaced (b) and more elliptical (c) than were those at junctions or bases of *S. pistillata* fragments. Several known biomineralization genes were DE, shown as $\log_2$FC between branch tips (positive values) and bases (negative values) (d) and $\log_{10}$FPKM along the branch axis (e) to clarify genes with high versus low expression. Only significantly DE genes are shown ($p<0.05$).

Figure 5. Schematic of environmental parameters (e.g., flow and light intensity, left) and resulting differential gene expression patterns and physiological outcomes for key processes

focusing on those enhanced at branch tips (right). We cannot assign gene expression to specific tissue layers or cell types in most cases, except for the likely localization of toxin and biomineralization genes to the oral ectoderm and calicoderm, respectively.

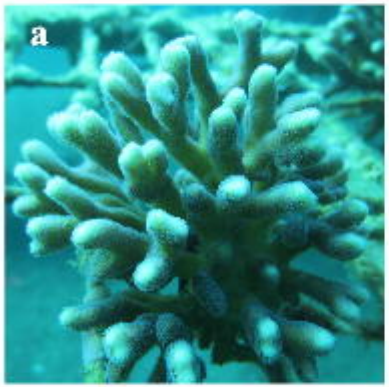
a

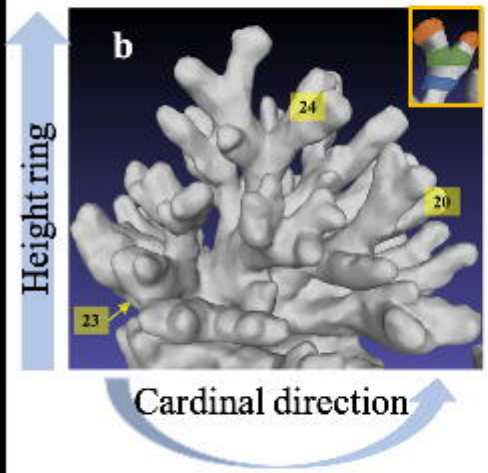
b
24
20
23
Height ring
Cardinal direction

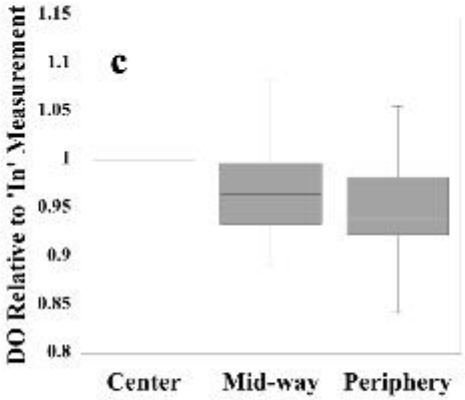
c
DO Relative to 'In' Measurement
1.15
1.1
1.05
1
0.95
0.9
0.85
0.8
Center
Mid-way
Periphery

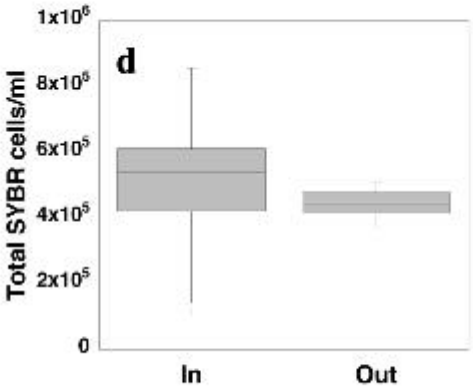
d
Total SYBR cells/ml
1x10^6
8x10^5
6x10^5
4x10^5
2x10^5
0
In
Out

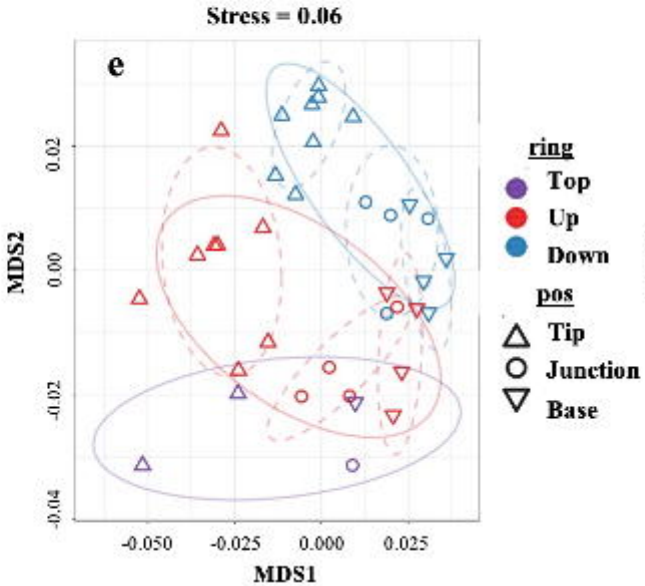
Stress = 0.06
e
MDS2
0.02
0.00
-0.02
-0.04
-0.050
-0.025
0.000
0.025
MDS1
ring
Top
Up
Down
pos
Tip
Junction
Base

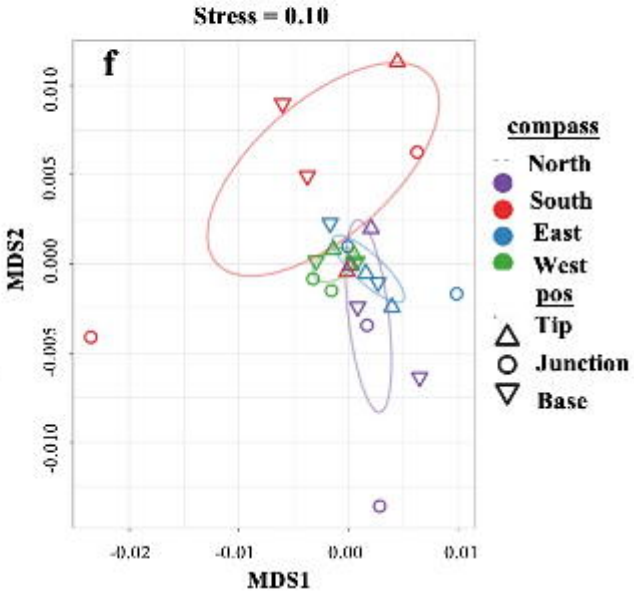
Stress = 0.10
f
MDS2
0.010
0.005
0.000
-0.005
-0.010
-0.02
-0.01
0.00
0.01
MDS1
compass
North
South
East
West
pos
Tip
Junction
Base

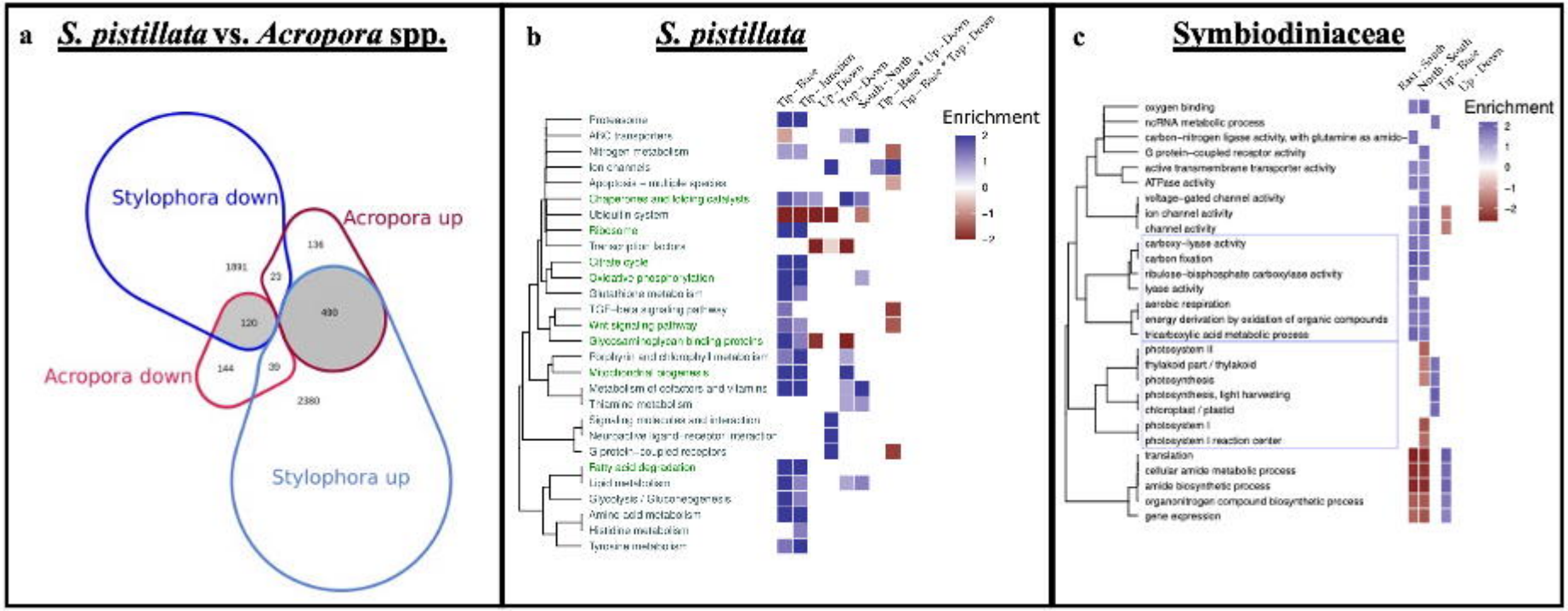
a
S. pistillata vs. Acropora spp.
Stylophora down
Acropora up
Acropora down
Stylophora up
1891
136
23
120
490
144
39
2380
b
S. pistillata
Tip - Base
Tip - Junction
Up - Down
Top - Down
South - North
Tip - Base * Up - Down
Tip - Base * Top - Down
Enrichment
2
1
0
−1
−2
Proteasome
ABC transporters
Nitrogen metabolism
Ion channels
Apoptosis – multiple species
Chaperones and folding catalysts
Ubiquitin system
Ribosome
Transcription factors
Citrate cycle
Oxidative phosphorylation
Glutathione metabolism
TGF-beta signaling pathway
Wnt signaling pathway
Glycosaminoglycan binding proteins
Porphyrin and chlorophyll metabolism
Mitochondrial biogenesis
Metabolism of cofactors and vitamins
Thiamine metabolism
Signaling molecules and interaction
Neuroactive ligand-receptor interaction
G protein-coupled receptors
Fatty acid degradation
Lipid metabolism
Glycolysis / Gluconeogenesis
Amino acid metabolism
Histidine metabolism
Tyrosine metabolism
c
Symbiodiniaceae
East - South
North - South
Tip - Base
Up - Down
Enrichment
2
1
0
−1
−2
oxygen binding
ncRNA metabolic process
carbon–nitrogen ligase activity, with glutamine as amido–
G protein–coupled receptor activity
active transmembrane transporter activity
ATPase activity
voltage–gated channel activity
ion channel activity
channel activity
carboxy–lyase activity
carbon fixation
ribulose–bisphosphate carboxylase activity
lyase activity
aerobic respiration
energy derivation by oxidation of organic compounds
tricarboxylic acid metabolic process
photosystem II
thylakoid part / thylakoid
photosynthesis
photosynthesis, light harvesting
chloroplast / plastid
photosystem I
photosystem I reaction center
translation
cellular amide metabolic process
amide biosynthetic process
organonitrogen compound biosynthetic process
gene expression

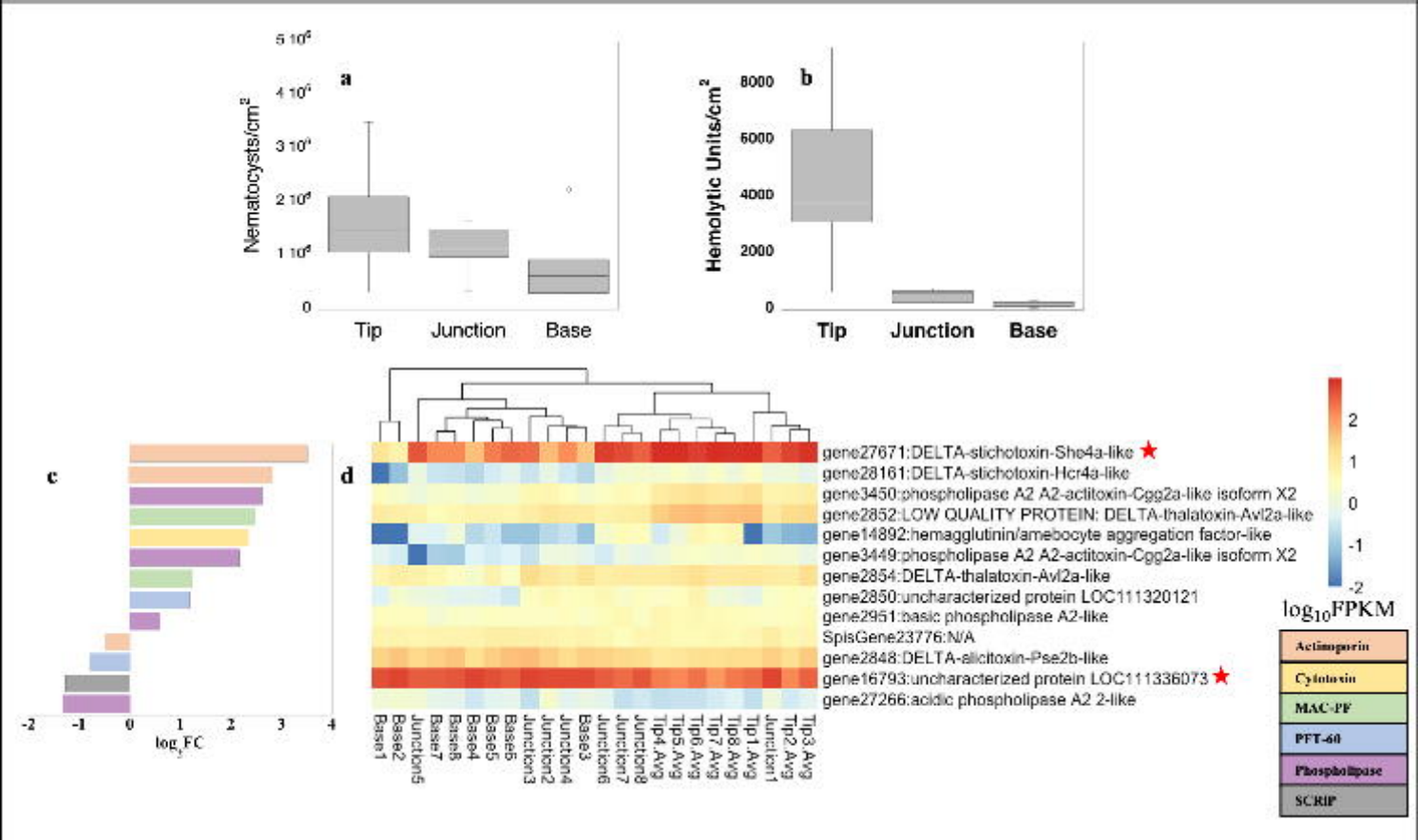
a
Nematocysts/cm²
5 10⁶
4 10⁶
3 10⁶
2 10⁶
1 10⁶
0
Tip
Junction
Base
b
Hemolytic Units/cm²
8000
6000
4000
2000
0
Tip
Junction
Base
c
log₂FC
-2
-1
0
1
2
3
4
d
gene27671:DELTA-stichotoxin-She4a-like
gene28161:DELTA-stichotoxin-Hcr4a-like
gene3450:phospholipase A2 A2-actitoxin-Cgg2a-like isoform X2
gene2852:LOW QUALITY PROTEIN: DELTA-thalatoxin-Avl2a-like
gene14892:hemagglutinin/amebocyte aggregation factor-like
gene3449:phospholipase A2 A2-actitoxin-Cgg2a-like isoform X2
gene2854:DELTA-thalatoxin-Avl2a-like
gene2850:uncharacterized protein LOC111320121
gene2951:basic phospholipase A2-like
SpisGene23776:N/A
gene2848:DELTA-alicitoxin-Pse2b-like
gene16793:uncharacterized protein LOC111336073
gene27266:acidic phospholipase A2 2-like
Base1
Base2
Junction5
Base7
Base4
Base5
Base6
Junction3
Junction2
Junction4
Base3
Junction6
Junction7
Junction8
Tip4.Avg
Tip5.Avg
Tip6.Avg
Tip7.Avg
Tip8.Avg
Tip1.Avg
Junction1
Tip2.Avg
Tip3.Avg
2
1
0
-1
-2
log₁₀FPKM
Actinoporin
Cytotoxin
MAC-PF
PFT-60
Phospholipase
SCRIP

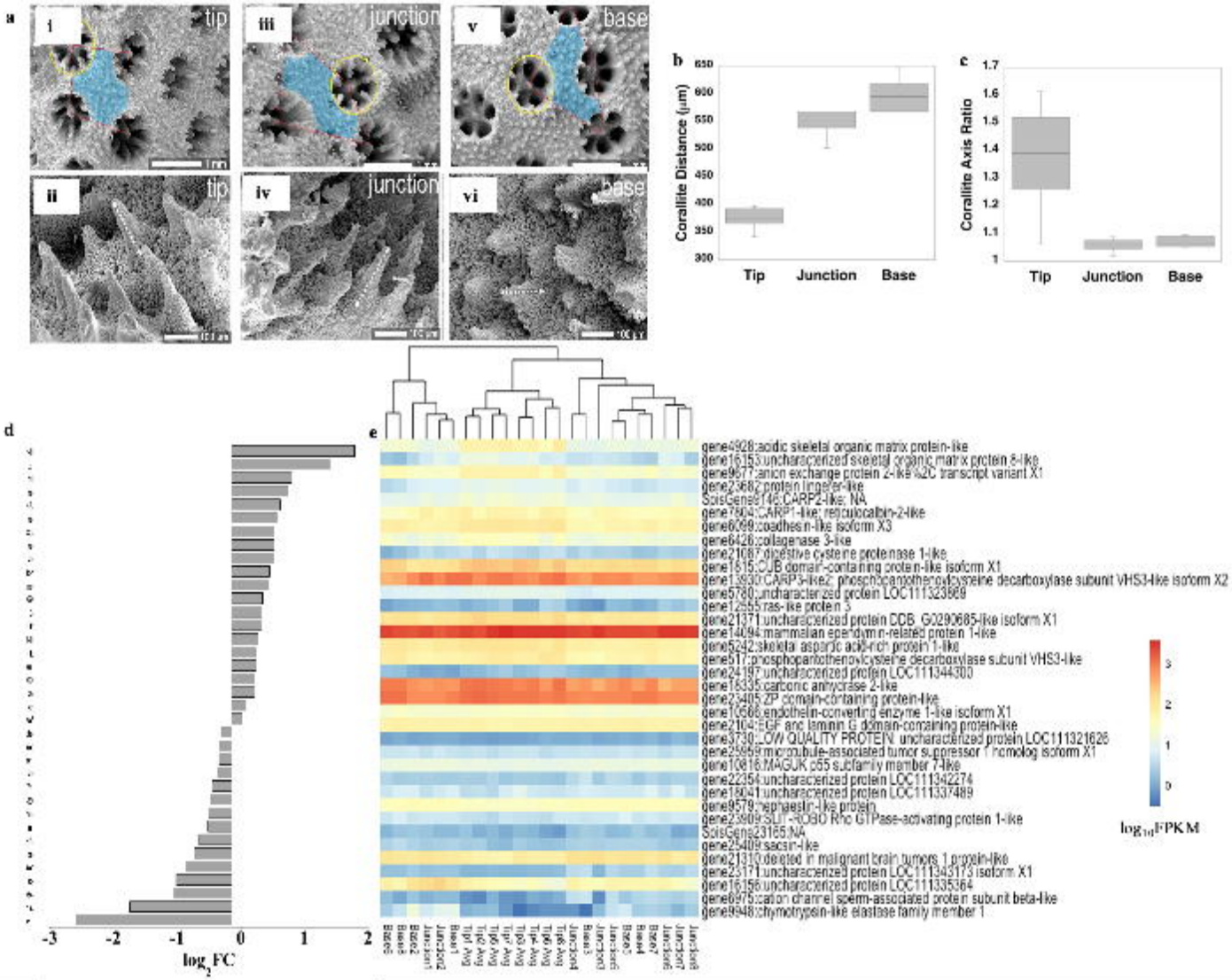

a
i
tip
iii
junction
v
base
ii
tip
iv
junction
vi
base
b
Corallite Distance (μm)
650
600
550
500
450
400
350
300
Tip
Junction
Base
c
Corallite Axis Ratio
1.7
1.6
1.5
1.4
1.3
1.2
1.1
1
Tip
Junction
Base
d
-3
-2
-1
0
1
2
log2FC
e
gene4928:acidic skeletal organic matrix protein-like
gene16153:uncharacterized skeletal organic matrix protein 8-like
gene9677:anion exchange protein 2-like %2C transcript variant X1
gene23682:protein lingerer-like
SpisGene8146:CARP2-like; NA
gene7804:CARP1-like; reticulocalbin-2-like
gene6099:coadhesin-like isoform X3
gene6426:collagenase 3-like
gene21087:digestive cysteine proteinase 1-like
gene1815:CUB domain-containing protein-like isoform X1
gene13930:CARP3-like2; phosphopantothenoylcysteine decarboxylase subunit VHS3-like isoform X2
gene5780:uncharacterized protein LOC111323869
gene12555:ras-like protein 3
gene21371:uncharacterized protein DDB_G0290685-like isoform X1
gene14094:mammalian ependymin-related protein 1-like
gene5242:skeletal aspartic acid-rich protein 1-like
gene517:phosphopantothenoylcysteine decarboxylase subunit VHS3-like
gene24197:uncharacterized protein LOC111344300
gene16335:carbonic anhydrase 2-like
gene23405:ZP domain-containing protein-like
gene10566:endothelin-converting enzyme 1-like isoform X1
gene2104:EGF and laminin G domain-containing protein-like
gene3730:LOW QUALITY PROTEIN: uncharacterized protein LOC111321626
gene25959:microtubule-associated tumor suppressor 1 homolog isoform X1
gene10816:MAGUK p55 subfamily member 7-like
gene22354:uncharacterized protein LOC111342274
gene18041:uncharacterized protein LOC111337489
gene9579:nephaestin-like protein
gene23909:SLIT-ROBO Rho GTPase-activating protein 1-like
SpisGene23165:NA
gene25409:sacsin-like
gene21310:deleted in malignant brain tumors 1 protein-like
gene23171:uncharacterized protein LOC111343173 isoform X1
gene16156:uncharacterized protein LOC111335364
gene6975:cation channel sperm-associated protein subunit beta-like
gene9948:chymotrypsin-like elastase family member 1
3
2
1
0
log10FPKM

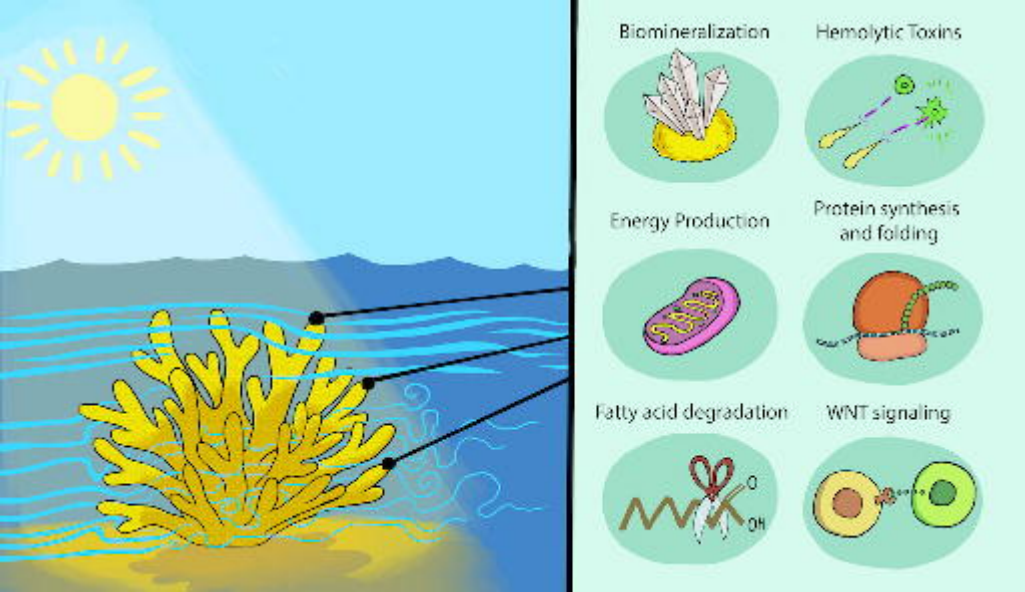
Biomineralization
Hemolytic Toxins
Energy Production
Protein synthesis and folding
Fatty acid degradation
WNT signaling
O
OH